Sustainable Food Technology

ROYAL SOCIETY OF CHEMISTRY

PAPER

View Article Online
View Journal | View Issue

Cite this: *Sustainable Food Technol.*, 2025, **3**, 2134

Omega-3 incorporation effects on the structural, rheological, and sensory properties of 3D-printed chocolate

Ruoyao Li,[a] Sushil Koirala,[a] Sangeeta Prakash,[a] Yun Xu[b] and Bhesh Bhandari*[a]

Omega-3 fatty acids are recognised for their health benefits but their incorporation into foods is limited by oxidative instability and undesirable sensory attributes. 3D food printing offers a potential solution by enabling precise spatial deposition and structural design to improve stability and product quality. This study examined the effects of two fortification forms, free oil and microencapsulated powder, at three concentrations (5%, 10%, 15%), on the physicochemical characteristics of 3D-printed dark chocolate. Particular emphasis was placed on microencapsulated formulations, with additional evaluation of sensory properties, storage stability, and their capacity to achieve nutritional enhancement while maintaining product integrity and acceptability.Results demonstrated that both form and concentration of omega-3 significantly influenced crystallisation behaviour (ΔH increased from 44.30 ± 1.69 J g^{-1} in the control to 57.66 ± 2.02 J g^{-1} in OP15, $p < 0.05$), texture (breaking force decreased from 84.46 ± 3.99 N in the control to 48.14 ± 4.14 N in OP15 and 25.86 ± 5.14 N in OO15), and rheological behaviour (OP15 exhibited the highest initial viscosity). Compared with oil, microencapsulated omega-3 showed superior compatibility with the chocolate matrix, enhancing crystallisation and shape fidelity. Sensory analysis revealed that OP10 achieved comparable overall acceptability to the control when fresh, although flavour scores decreased significantly after two months of storage at 25 °C. Overall, fortification of omega-3 at moderate levels (5–10%), combined with optimised printing conditions, provides an effective strategy to improve nutritional value, structural performance, and consumer acceptance of functional 3D-printed chocolate.

Received 14th August 2025
Accepted 13th September 2025

DOI: 10.1039/d5fb00475f

rsc.li/susfoodtech

Sustainability spotlight

This study advances sustainable food design by integrating omega-3 fortification with 3D food printing to produce nutrient-dense chocolate. By altering fortification levels to meet specific dietary needs, this approach minimises nutrient waste and supports personalised nutrition. The fortification of omega-3 enhances oxidative stability, potentially extending shelf life and reducing product losses during distribution and storage. Extrusion-based 3D printing facilitates localised manufacturing with flexible formulation control therby lowering transportation requirements and associated emissions. This method also reduces packaging requirements through precise portion fabrication, improving resource efficiency. These combined benefits align with sustainable production principles, contributing to healthier diets while reducing the environmental footprint of functional food manufacturing.

1. Introduction

Functional foods have gained significant attention as a strategic approach to combat the global rise in non-communicable diseases, particularly those associated with poor dietary patterns, such as cardiovascular disease, metabolic syndrome, and neurodegenerative conditions.[1,2] Unlike conventional food products, functional foods are formulated to deliver targeted physiological effects beyond basic nutrition by incorporating bioactive compounds that modulate biological processes.[3–5] Among the most extensively researched functional bioactives are omega-3 long-chain polyunsaturated fatty acids (LC-PUFAs), especially eicosapentaenoic acid (EPA) and docosahexaenoic acid (DHA).[6,7] These fatty acids are critical components of neural and retinal membranes, and their dietary intake has been strongly correlated with a reduced risk of atherosclerosis, chronic inflammation, and cognitive decline.[6,8,9] DHA, in particular, is essential during fetal and neonatal development and is a principal component of breast milk.[10] Yet, endogenous conversion from α-linolenic acid (ALA) is limited in humans (<0.5% for DHA), and direct dietary supplementation of DHA has become an effective way to meet this requirement.[11] Emerging clinical evidence has also linked sustained maternal

[a]*School of Agriculture and Food Sustainability, The University of Queensland, Brisbane, 4072, QLD, Australia. E-mail: b.bhandari@uq.edu.au*
[b]*Research and Development Department, Nu-Mega Ingredients Pty Ltd, Brisbane, QLD, Australia*

DHA intake to improved infant neurocognitive outcomes and a reduced risk of postpartum depression.[10,12,13] Although maternal plasma DHA levels show a significant and prolonged downward trend in the early postpartum period, this change can be ameliorated by adequate dietary DHA supplementation.[10] An effective and convenient supplementation method would ensure that nursing mothers obtain adequate EPA and DHA to support both maternal health and infant development, while also benefiting children and the general population by improving omega-3 intake across all age groups.

However, the integration of EPA and DHA into food matrices is limited by their high susceptibility to oxidation due to the presence of multiple unsaturated double bonds. Lipid peroxidation not only degrades nutritional quality but also generates volatile aldehydes and ketones that compromise sensory acceptability.[11] This oxidative instability poses a significant challenge in formulating omega-3 fortified products. To mitigate these limitations, various technological interventions have been developed, with microencapsulation emerging as the most widely adopted approach. Microencapsulation involves entrapping lipophilic compounds within protective wall materials, often *via* spray-drying or complex coacervation, effectively reducing oxygen exposure and masking undesirable flavours.[12,13] Additionally, encapsulated forms enhance ingredient dispersion, facilitate controlled release during digestion, and improve shelf stability, making them suitable for a diverse range of food applications.

The advancement of digital food manufacturing, particularly extrusion-based three-dimensional (3D) food printing, presents an opportunity to integrate bioactive compounds, such as omega-3s, into structurally and nutritionally customisable food matrices.[14–16] 3D food printing enables the layer-by-layer fabrication of food structures with precise spatial control over ingredient placement, allowing for novel geometries, textures, and nutrient compositions.[17–19] Chocolate is a promising candidate for omega-3 delivery *via* extrusion-based 3D printing due to its unique thermo-mechanical behaviour and oxidative stability.[20] Composed of sugar and cocoa particles dispersed in a continuous fat phase (primarily cocoa butter), chocolate exhibits thermoplastic behaviour upon gentle heating and solidifies rapidly on cooling, making it ideal for melt-based deposition.[21] The composition of chocolate creates an environment with low water activity, low oxygen, and low permeability, which can further inhibit oxidative reactions, offering a protective medium for polyunsaturated lipids.[22] The intense flavour of chocolate also helps mask fishy or metallic off-notes associated with marine-derived omega-3s. However, introducing foreign lipids or encapsulated powders may significantly affect chocolate's flow characteristics, particle dispersion, and crystallisation kinetics. Maintaining the stable β(V) polymorph of cocoa butter (a metastable crystalline form with a melting point of ~33–34 °C, responsible for gloss, snap, and desirable mouthfeel) is critical to achieving desirable texture, gloss, and snap; uncontrolled lipid addition may disrupt this polymorphic equilibrium, leading to fat bloom, inferior texture, and reduced shelf life.[23,24] Consequently, understanding the interaction between the omega-3 delivery form and chocolate rheology during printing is essential to preserve both the functional and sensory qualities.

There are very limited studies on the microencapsulation of omega-3 using 3D food printing technology. Although some studies have explored the possibility of omega-3 fortification in chocolate, most have focused on either oil or powder forms at a single concentration, often without assessing performance under 3D printing conditions.[20,25–28] There remains a lack of systematic research evaluating how different omega-3 forms and concentrations affect printability, rheological behaviour, microstructure, and sensory acceptance in printed chocolate systems.

Therefore, the primary objective of this study is to develop omega-3 incorporated 3D printed functional chocolate. In addition to that, it aims to study the effects of omega-3 fatty acid enrichment, using both liquid fish oil and microencapsulated powder, at three concentrations (5%, 10%, 15% w/w) on the physicochemical, rheological, thermal, structural, and sensory properties of 3D-printed dark chocolate. These concentrations were selected to simulate real-world nutritional applications, from low-dose paediatric intake to high-dose lactating women and cardiovascular support. By linking omega-3 bioefficacy with emerging digital food technologies, this study supports the development of next-generation functional foods that are both nutritious and technologically feasible through precision manufacturing.

2. Materials and methods

2.1 Preparation of base chocolate ink

The printing material (ink) was prepared using commercially available Belgian dark block chocolate (85% cocoa solids) purchased from a local supermarket. To prepare the ink, chocolate was first grated using a manual food grater (model 35045, Microplane®, Grace Manufacturing Inc., USA). The mixture was thoroughly blended using a high-speed blender (model HR3652, Philips, Koninklijke Philips N.V., Netherlands).

2.2 Fortification with omega-3 fatty acids

Two types of omega-3 ingredients from Nu-Mega Ingredients (**https://www.nu-mega.com/en/**) (Brisbane, Australia) were incorporated for fortification:

- Driphorm® HA DHA-S 200 microencapsulated powder (containing 48% algal oil; 200 mg per g DHA + 7 mg per g EPA, median particle size $d(0.5) \approx 149$ μm) and
- HiDHA® Algal oil (containing 400 mg per g DHA).

Each 3D-printed chocolate piece weighed approximately 3.5 g. Fortification levels were set at 5%, 10%, and 15% (w/w), corresponding to 0.175 g, 0.35 g, and 0.525 g of omega-3 supplement per piece, respectively. The effective omega-3 content was calculated as:

$$\text{Effective content (mg)} = \text{potency (mg g}^{-1}) \times \text{supplement mass (g)}$$

For Driphorm® HA DHA-S 200 powder (207 mg per g DHA + EPA), this yielded 36.2, 72.5, and 108.7 mg per piece, equivalent

Table 1 Sample codes for the fortified chocolate formulations

Omega-3 sources	0% addition (control)	5% addition	10% addition	15% addition
Driphorm® HA DHA-S 200 (OP)	Control	OP5	OP10	OP15
HiDHA® Algal oil (OO)	Control	OO5	OO10	OO15

to 0.25×, 0.50×, and 0.75× the recommended adequate intake (AI). For HiDHA® algal oil (400 mg per g DHA), the corresponding values were 70, 140, and 210 mg, equal to 0.48×, 0.97×, and 1.45× AI. These calculations confirm that the stated mg values (72.5, 145, and 217.5 mg) result directly from multiplying the supplement proportion by the 3.5 g piece weight and the known ingredient potency.

2.3 Chocolate tempering and formulation coding

The grated and fortified chocolate formulation was melted in a 45 °C water bath (Thermoline Scientific, Sydney, NSW, Australia) according to the method described by ref. 29 with some modifications. Samples were then tempered *via* a two-stage method before printing: cooling to 27–28 °C to induce crystallisation and generate nuclei, including the target β(V) polymorph, followed by reheating to 30–31 °C to melt unstable crystal forms with lower melting points (*e.g.*,β(IV)) while retaining β(V) crystals. Final sample codes were defined by ingredient type and addition level (Table 1). "OP" refers to samples fortified with the Driphorm® powder, while "OO" refers to samples containing the algal oil. The numeric suffix indicates the percentage of omega-3 addition. "Control" denotes samples without omega-3.

2.4 Design and 3D printing of chocolate

2.4.1. 3D geometry design. A chocolate model, 1, with 24 mm × 24 mm dimensions and 6 mm thickness, was designed using Tinkercad online 3D modeling software. These dimensions were chosen to match standard commercial chocolate block sizes in order to ensure consumer familiarity and make the sensory evaluation results practically relevant.

2.4.2. Slicing. The 3D model created using the online software was exported in *.stl* format and imported into Repetier-Host software for slicing, utilizing the Slic3r module, which generates the final g-code for the printing process. The shell perimeters were set to default at three shells (~2.34 mm thickness), considering the inner nozzle diameter is 1.4 mm. A rectilinear infill pattern with an infill of 100% was set for the printing process.

2.5 3D printing

A Shinnove 3D printer (model Shinnove-D1, Hangzhou Shiyin Technology Co., Ltd, China) was used in this study. This printer was equipped with a syringe-based extrusion system equipped with two independently controlled syringe barrels (60 mL), each surrounded by a heating jacket. The printing temperature was set to 30 °C, which provided sufficient fluidity for steady extrusion while avoiding the complete melting of the chocolate's crystalline structure. The printing parameters were optimised as per ref. 30. All printed samples were kept under refrigeration at around 8 °C until the execution of textural analysis and sensory evaluation.

2.6 Analysis

2.6.1. Rheological characterisation of 3D-printed chocolate. The flow behaviour of the tempered chocolate (prior to printing) was evaluated using an AR-G2 rheometer (TA Instruments, USA) with a 40 mm sand-blasted parallel plate geometry at room temperature (25 °C). A peak hold test was performed in controlled shear rate mode, following the method described by ref. 31. A constant shear rate of 100 s^{-1} was applied for 10 min, and the viscosity was recorded as a function of time to observe any viscosity breakdown or stabilisation under shear. Each sample formulation was tested in replicates to ensure repeatability of the rheological data.

2.6.2. Texture analysis of 3D-printed chocolate. The textural properties (hardness) of the 3D-printed chocolates were measured according to the method of ref. 32 and 33. A TA.XT Plus texture analyser (Stable Micro Systems, UK) equipped with a Warner–Bratzler blade probe and controlled by Exponent software (v6.1.9.0) was used. Tests were carried out at ambient temperature (22–23 °C). Each chocolate sample was positioned vertically under the blade to prevent sample sliding during the test. A compression (cutting) test was then performed with a 10 mm penetration distance. The test parameters were as follows: pre-test speed, 1.0 mm s^{-1}; test speed, 2.0 mm s^{-1}; post-test speed, 10.0 mm s^{-1}; and trigger force, 5 g. Three pieces from each of the control, OO, and OP groups were analysed, and the maximum force (breaking force in newtons, N) required to cut through each sample was recorded for texture analysis.

2.6.3. Thermal property analysis of 3D-printed chocolate. The thermal behaviour of the printed chocolates was analysed using DSC (DSC 1, STARe 143 System, Mettler Toledo), based on the method of ref. 30 with modifications for post-print samples. A DSC 1 STARe system (Mettler Toledo, Switzerland) was used. Approximately 5.5–6.5 mg of chocolate from each sample was sealed in a 40 μL aluminium pan and equilibrated at 25 °C, and then heated to 50 °C at a rate of 2 °C min^{-1} under a nitrogen purge. The thermal curve was recorded, and the onset (T_o), peak temperature (T_p), and endset temperature (T_c) were determined. The melting enthalpy (ΔH, in J g^{-1}) was calculated from the area under the endothermic peak, as well as the temperatures T_o and T_c. To account for the dilution effect of the added omega-3 materials on the chocolate mass, the ΔH values for enriched samples were adjusted based on the fraction of chocolate in the sample, so that the corrected ΔH reflects the crystallisation

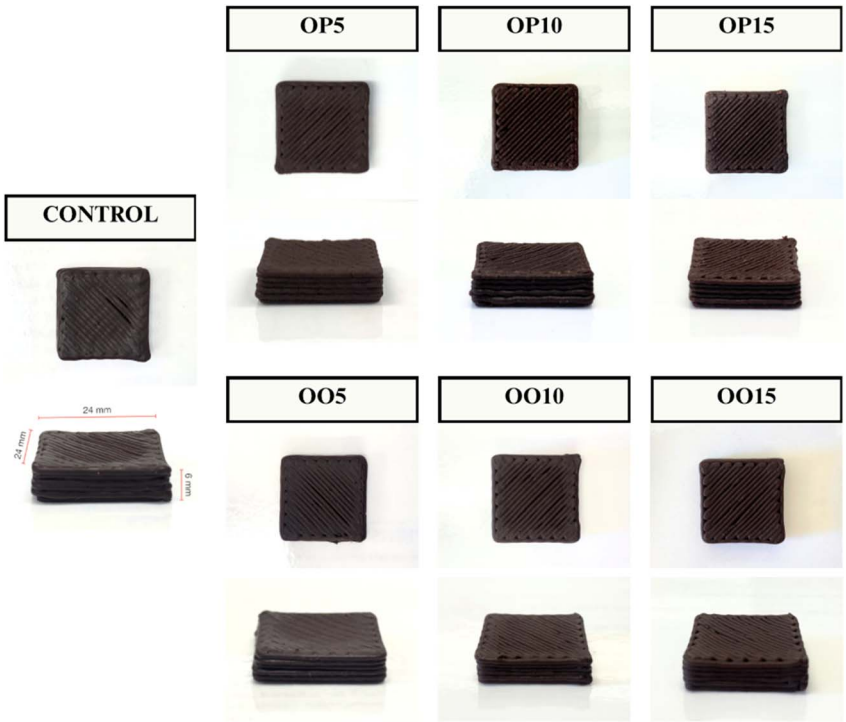

Fig. 1 3D-printed dark chocolate samples with control, powder-based (OP) and oil-based (OO) omega-3 at 5%, 10%, and 15% (w/w) concentrations.

degree of the cocoa butter phase. At least three replicate measurements were performed for each sample formulation to ensure reliability of the thermal data.

2.6.4. Microscopic observation of 3D-printed chocolate. The surface microstructure of the printed chocolates (before and after storage) was examined using an optical microscope (Leica DM2500, Leica Microsystems, Germany). Images were captured with Leica Application Suite (LAS) v4.7 software. One piece from each formulation group (control, OP5, OP10, OP15, OO5, OO10, OO15) was stored at 22 °C for two months to observe the development of fat bloom and to examine the surface microstructure of the sample. All samples were observed under identical conditions using a Type I filter and a 5× objective lens.

2.7 Sensory evaluation of 3D-printed chocolate

Sensory evaluation was conducted to assess consumer preference and acceptability of control *versus* OP10 chocolate samples. OP10 (10% microencapsulated omega-3) was chosen because it represented the medium fortification level, showed good structural stability and processing adaptability in earlier analyses, and served as a benchmark for optimisation. This design allowed us to establish whether consumer acceptance at the medium level was sufficient to justify higher fortification (OP15) or, if necessary, to reduce to a lower level (OP5).

All evaluations were performed in the sensory analysis laboratory at the University of Queensland (Brisbane, Australia) using RedJade software, with prior ethics approval. Participants were semi-trained volunteers (students and staff from the Food Engineering department, mixed gender distribution) who received a standardised briefing to ensure consistency in evaluation procedures and terminology.

The study was carried out in two independent sessions with different objectives: Session 1 ($n = 36$) used a paired-comparison test to capture immediate preferences in aroma, flavour, and overall liking of freshly printed samples; Session 2 ($n = 31$) was conducted after two months of ambient storage using a structured Likert scale to evaluate changes in aroma, taste, and flavour acceptability. Sample presentation order was counterbalanced (control → OP10 *vs.* OP10 → control) to minimise order bias, and panellists were instructed to cleanse their palate between samples.

2.8 Statistical analysis

All data were reported as mean ± standard deviation (SD). Statistical analyses were performed using GraphPad Prism version 10.0.2 (GraphPad Software, LLC, San Diego, CA, USA). Instrumental data were analysed by one-way analysis of variance (ANOVA) followed by Tukey's *post hoc* test. Sensory preference data from Session 1, collected as binary paired-comparison choices, were evaluated using a two-tailed binomial test. For Session 2, participants rated aroma, flavour, and taste on a 9-point Likert scale. Before formal statistical testing, normality was assessed using the Shapiro–Wilk test, and homogeneity of variance was assessed using Levene's test. The results showed no significant differences ($p > 0.05$), indicating that the data met the prerequisites for parametric testing. Therefore, a paired *t*-

test was used to compare differences between the control and OP10 groups. Significance was set at $p < 0.05$.

3. Results and discussion

3.1 Appearance and printing performance of 3D printed chocolate

The visual appearance and printability of control and omega-3-fortified chocolate samples are shown in Fig. 1. All formulations, regardless of omega-3 type (oil or powder) and concentration (5%, 10% or 15%), were successfully printed using identical extrusion parameters, resulting in uniform, stable printed forms. This demonstrates the suitability of dark chocolate as a suitable matrix for extrusion-based food printing, even with omega-3 fortification. The inherent melting and solidification properties of dark chocolate support precise shaping, which aligns with previous reports on its printability.[34] Notably, no formulation led to nozzle clogging, loss of shape fidelity, or structural collapse, demonstrating consistent printability. Such reliability is essential in functional food printing, where print defects can affect consumer acceptance and nutrient delivery.[35]

While all sample groups exhibited similar macrostructure, notable differences were observed in surface quality. The control samples displayed a smooth and glossy appearance of well-tempered dark chocolate. In contrast, the chocolate in the OP group exhibited a progressively rougher texture and matte finish with increasing concentration. Previous studies have reported that the microstructure and particle arrangement of chocolate affect appearance attributes such as surface gloss.[36,37] The incorporation of microencapsulated omega-3 likely intensified particle–particle interactions in the system and disrupted the continuity of the fat matrix, contributing to microstructural disorder and reduced surface smoothness.[29] By comparison, samples in the OO group (containing liquid omega-3) suggest better miscibility and structural integration of the oil into the lipid phase. These findings highlight the critical influence of the physical form of omega-3 addition (solid microcapsules *vs.* liquid oil droplets) on the final surface texture and gloss of the printed chocolate.

3.2 Microstructural analysis

Microscopic analysis (Fig. 2) further highlighted the impact of omega-3 fortification on chocolate microstructure. Control and OO samples exhibited uniform, compact surfaces without detectable inclusions, suggesting effective dispersion of omega-3 oil without phase separation or voids. In contrast, OP10 and OP15 samples revealed localised white aggregates, indicative of poorly dispersed microencapsulated omega-3. Quantitative image analysis showed that the average aggregate size increased significantly from <10 μm in control and OO samples to 28.4 ± 3.1 μm in OP10 and 45.2 ± 6.3 μm in OP15 ($p < 0.05$). The surface coverage of visible aggregates also rose from 2.1% in OP5 to 18.7% in OP15, confirming concentration-dependent disruption of surface uniformity. This behaviour may be attributed to reduced free fat content and enhanced particle–particle interactions, which increase system viscosity and limit dispersibility.[29,38]

The frequency and size of these aggregates increased with higher powder loading, in agreement with the macroscopic surface observations. This behaviour may be attributed to reduced free fat content and enhanced particle–particle interactions, which increase system viscosity and limit dispersibility.[29,38] These findings demonstrate that when fortification exceeds 10%, aggregate prevalence surpasses the critical threshold of 15% surface coverage, which is likely to compromise both appearance and texture. These effects are exacerbated as the concentration of microencapsulated omega-3 increases, where inconsistencies in flow between solid microcapsules and molten chocolate may drive particle migration toward the surface.[39,40] Thus, formulation design must consider the trade-off between structural uniformity and functional stability in omega-3-enriched 3D printed chocolate systems.

3.3 Texture analysis

Texture measurements (Fig. 3 and Table 2) revealed a general softening effect in all omega-3-fortified samples compared to the control. This effect was most pronounced in oil-fortified chocolates (OO group), which exhibited a dose-dependent

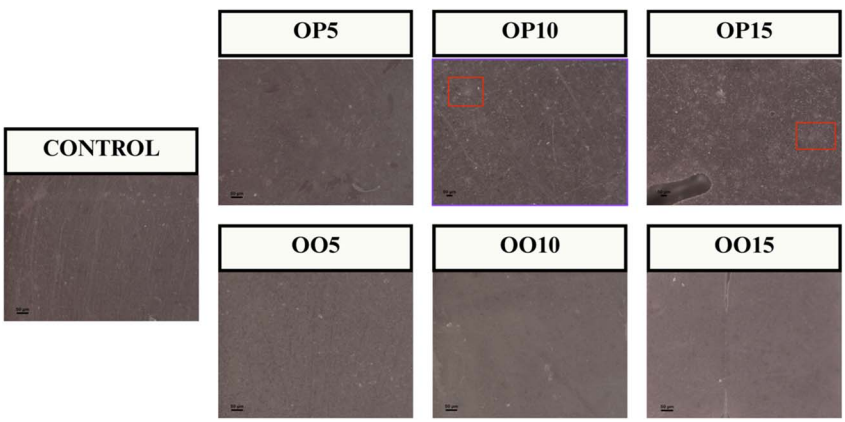

Fig. 2 Microscopic surface images of control and omega-3-fortified chocolate samples. OP10 and OP15 samples show visible particle aggregation, while control and OO samples exhibit smooth, uniform surfaces. Scale bar = 100 μm.

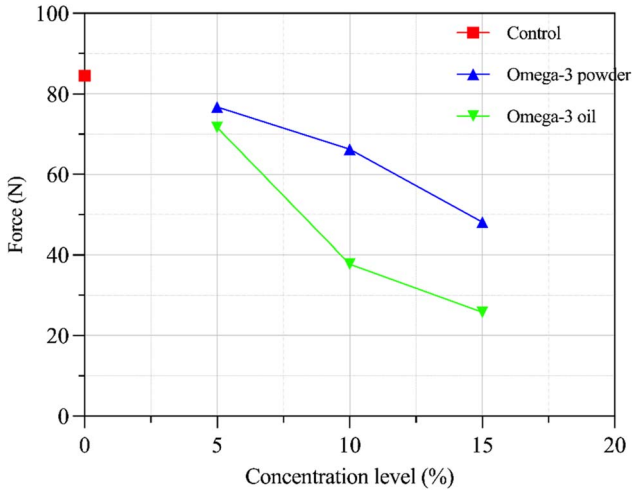

Fig. 3 Texture (hardness) of chocolates fortified with omega-3 powder and oil at varying concentrations.

Table 2 Breaking force (N) of 3D-printed chocolate samples with different forms and levels of omega-3[a]

Sample	Force (N)
Control	$84.46 \pm 3.99^{(a)}$
OP5%	$76.80 \pm 6.33^{(a)(b)}$
OP10%	$66.26 \pm 4.44^{(b)}$
OP15%	$48.14 \pm 4.14^{(c)}$
OO5%	$71.68 \pm 1.33^{(b)}$
OO10%	$37.70 \pm 2.75^{(c)(d)}$
OO15%	$25.86 \pm 5.14^{(d)}$

[a] Mean values of force (N) bearing different superscript letters are significantly different ($p < 0.05$).

decrease in hardness. The inclusion of liquid fats disrupts cocoa butter's crystalline network, diluting solid fat content and interfering with crystallisation, resulting in a structurally weaker, less cohesive network.[41,42] This is consistent with the findings by the authors of ref. 25, who noted that the addition of liquid omega-3 significantly induced a more pronounced softening effect on chocolate than in solid granular form. Our results further confirmed that liquid omega-3 indeed has a more pronounced softening effect on chocolate.

Chocolates fortified with microencapsulated omega-3 powder (OP group) exhibited comparatively milder reductions in hardness. Notably, at the lowest concentration (OP5), the texture remained statistically similar to that of the controls ($p > 0.05$), suggesting minimal disruption to cocoa butter crystallisation at this level. At higher concentrations (OP10 and OP15), hardness reductions were apparent but remained less severe compared to those of oil-fortified samples, indicating a concentration threshold above which structural integrity notably decreases. The authors of ref. 29 similarly observed that low concentrations of microcapsules might reinforce the chocolate structure by acting as inert fillers. Consequently, microencapsulation enables higher omega-3 fortification without significantly compromising the chocolate's texture compared to liquid oil.

Table 2 shows the changes in the average fracture force (N) of 3D printed chocolate samples under different addition forms (microcapsule powder and oil) and addition amounts (5%, 10%, 15%), which further supports the findings of Fig. 3 at the numerical level and reveals the advantage of the microcapsule powder group in maintaining structural stability at low addition amounts. The results show that the control group had the highest average fracture force. As the amount of omega-3 added increased, the fracture force of the sample gradually decreased, and the OO group had a stronger interference effect on the cocoa butter crystal network due to a more significant decrease. It is worth mentioning that the average fracture force of the OP5 sample was not significantly different from that of the control group ($p > 0.05$), which indicates that omega-3 in the form of microcapsule powder will not cause significant damage to the chocolate structure at an addition amount of 5%. However, the fracture force of OP5 was not significantly different from that of OP10 and OO5 ($p > 0.05$), which indicates that the weakening effect of oil and microcapsule powder on hardness at an addition amount of 5% is at a similar level. Therefore, the 5% addition content caused OP5 to be in the stage of structural rigidity decline, meaning that the fat crystal was disturbed, but no significant or large-scale structural collapse had occurred. Thus, the 5% addition content caused OP5 to be in the critical interval of structural change, where the original chocolate structure was destroyed, but no significant and large-scale structural collapse had occurred. This trend suggests that the addition of low doses of omega-3 is insufficient to impact structural stability significantly, and the ability of microencapsulated omega-3 powder to reduce structural rigidity is limited compared to that of lipid omega-3.

Table 3 DSC data on onset (T_o), peak (T_p), and endset (T_c) temperatures, and enthalpy ΔH of 3D-printed chocolate samples with different levels of omega-3[a]

	T_o (°C)	T_p (°C)	T_c (°C)	ΔH (J g^{-1})
Control	$27.69 \pm 0.39^{(a)}$	$30.77 \pm 0.24^{(a)}$	$32.24 \pm 0.17^{(a)}$	$44.30 \pm 1.69^{(a)}$
OP5	$26.69 \pm 2.41^{(a)}$	$30.98 \pm 0.13^{(a)}$	$32.41 \pm 0.19^{(a)}$	$47.90 \pm 2.70^{(ab)}$
OP10	$25.25 \pm 0.12^{(a)}$	$30.84 \pm 0.41^{(a)}$	$32.11 \pm 0.14^{(a)}$	$52.28 \pm 4.44^{(bc)}$
OP15	$26.23 \pm 1.65^{(a)}$	$31.31 \pm 0.40^{(a)}$	$32.79 \pm 0.25^{(b)}$	$57.66 \pm 2.02^{(c)}$

[a] Mean values of onset (T_o), peak (T_p), and endset (T_c) temperaures, and enthalpy (ΔH, J g^{-1}) bearing different superscript letters are significantly different ($p < 0.05$).

3.4 Thermal properties

As shown in Table 3, the thermal properties of chocolates fortified with microencapsulated omega-3 powder remained largely stable across concentrations. The onset (T_o), peak (T_p), and endset (T_c) melting temperatures ranged from 25.25 to 27.69 °C, 30.77 to 31.31 °C, and 32.11 to 32.79 °C, respectively. Although T_c in the OP15 group was significantly higher than that of the control ($p < 0.05$), no consistent trend was observed in T_o or T_p across samples, indicating minimal disruption to cocoa butter crystallisation. The T_o and T_p values of the microencapsulated omega-3 samples at varying levels were not significantly different from those of the control group. Changes in T_c also fell within the range indicative of cocoa butter polymorph stability. Since different polymorphs have distinguishable melting characteristics, it can be inferred that the polymorphic types of the omega-3-fortified and control groups are consistent, and that the addition of omega-3s without microencapsulation did not induce the formation of unstable polymorphs.[43–45] Therefore, the added microencapsulated omega-3 powder has good lipid phase compatibility and crystallisation synergy with chocolate.

In contrast, the melting enthalpy (ΔH) exhibited a significant upward trend with increasing addition amount, rising from 44.30 J g^{-1} in the control group to 57.66 J g^{-1} in the OP15 group, and the difference between the groups was statistically significant ($p < 0.05$). This phenomenon indicates that microencapsulated omega-3 significantly affects the melting thermal behaviour of chocolate. This suggests enhanced crystallinity, likely due to the microcapsules acting as nucleation sites.[46] The authors of ref. 47 pointed out that solid particles in chocolate act as nucleation sites for the fat phase, helping to form crystals and thereby affecting the spatial distribution and crystallisation behaviour of the fat nuclei, potentially reducing the integrity of the network structure. Therefore, the addition of microencapsulated omega-3 will induce the formation of more crystals, thereby increasing crystallinity and melting energy requirements. However, the study by ref. 25 reported that the addition of both forms of omega-3 would lead to a decrease in ΔH, which is contrary to the results of this study. The differences may stem from multiple aspects – the properties of omega-3 powders and embedding wall materials from different sources may have distinct crystal formation mechanisms, thereby affecting the crystallisation behaviour. Additionally, this study employed a concentration gradient design rather than a single addition amount. The set concentration may be within the effective concentration range of inducing the nucleation mechanism and does not exceed the critical level that destroys the crystal network. Therefore, the added microencapsulated omega-3 powder not only does not interfere with the formation of cocoa butter crystals within a specific concentration range, but can also regulate crystal formation, which promotes crystallinity.

3.5 Rheological behaviour

The apparent viscosity–time profiles of chocolate samples under continuous shear (Fig. 4) demonstrated pronounced thixotropic behaviour, with a rapid initial viscosity drop followed by stabilisation, aligning with previous findings. At the onset of shear, the apparent viscosity of OP15 was 7.12 Pa s, representing a 71.9% increase over the control (4.14 Pa s). OP10 and OP5 also showed elevated initial viscosities of 6.29 and 4.94 Pa s, respectively. Initial viscosity followed the trend OP15 > OP10 > OP5 > control, indicating an increase in network strength and interparticle resistance with the addition of microencapsulated omega-3 fatty acids.

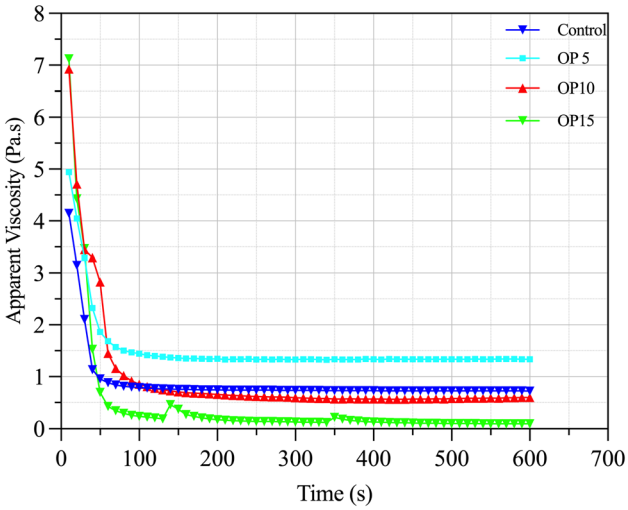

Fig. 4 Apparent viscosity (Pa s)–time (s) curves of chocolate samples with different amounts of microencapsulated omega-3 added under constant shear conditions.

At steady-state shear (plateau, from 110 s), viscosity stabilised at 0.15 ± 0.07 Pa s in OP15 and 0.61 ± 0.06 Pa s in OP10, which were lower than that of OP5 (1.34 ± 0.02 Pa s), suggesting a particle-induced lubrication mechanism at higher concentrations. OP5 maintained a higher plateau viscosity than the control, suggesting enhanced flow resistance yet stable printability. However, the viscosity of the OP10 and OP15 groups at the shear plateau was lower than that of the OP5 group and showed a downward trend with increasing addition amount, indicating that the flow resistance within the system decreased after the addition amount exceeded a certain level. This trend may be related to the particle-induced lubrication mechanism. We hypothesised that there may be a critical concentration value in the addition amount range of 5% to 10%, which refers to the particle-induced lubrication effect caused by high-concentration particles. Under this mechanism, high-addition content microencapsulated omega-3 particles may play a similar role in the shear process to traditional lubricants (such as magnesium stearate, MgST) in high-solid fat-based systems such as chocolate, that is, reducing friction and adhesion between particles and improving the lubricity of the material, thereby improving its flow stability during deposition or processing.[37] Repeated small viscosity oscillations (±0.2 Pa s fluctuations) were observed in OP15, further confirming microstructural instability under prolonged shear. This may be due to excessive particle concentration causing transient

Table 4 Percentage of participant preference for control and OP10 samples in terms of aroma, flavour, and overall liking in Session 1 ($n = 36$)[a]

	Aroma	Flavour	Overall
Control	47[(a)]	44[(a)]	44[(a)]
OP10	53[(a)]	56[(a)]	56[(a)]

[a] Percentages of participant preference for aroma, flavour, and overall liking bearing different superscript letters are significantly different ($p < 0.05$).

aggregation and reaggregation during the printing process. Therefore, while moderate addition levels (≤10%) enhanced rheological stability, excessively high concentrations induced periodic fluctuations that could compromise long-term print fidelity.

3.6 Sensory properties

Sensory acceptability is crucial for the commercial success of functional foods; therefore, the sensory attributes of the printed chocolates were assessed both immediately after production and following storage. In paired comparison tests of freshly printed samples (Table 4), omega-3 fortified chocolate containing 10% microencapsulated fish oil powder (OP10) was sensorially indistinguishable from control dark chocolate, with no statistically significant differences ($p > 0.05$) in aroma, flavour, or overall liking detected by panellists. This result indicates that the microencapsulation approach effectively masked potential fishy or off-flavours commonly associated with omega-3, preserving the classic sensory characteristics of dark chocolate. This observation aligns with previous findings by the authors of ref. 25, who reported that consumers prefer dark chocolate fortified with microencapsulated omega-3 over control forms due to the effective masking of off-flavours. The fresh samples retained typical desirable chocolate sensory notes such as roasted cocoa and mild bitterness, with no detectable off-notes reported by panellists.

However, after two months of ambient storage at approximately 25 °C, changes in the sensory profile of OP10 (microencapsulated omega-3 powder, 10% addition) became evident, although no alterations were observed in surface properties typically associated with fat or sugar bloom (Table 5). Aroma ($t = -0.2659$, df = 60, $p = 0.7913$) and taste ($t = -1.9606$, df = 60, $p = 0.0546$) of OP10 did not differ significantly from those of the control and remained acceptable. However, flavour was significantly lower in OP10 ($t = -2.7146$, df = 60, $p = 0.0087$). Panellists described the off-flavours as "stale" or "oxidised," indicating oxidative degradation of the omega-3 fatty acids within the microcapsules during storage. Omega-3 oils are well documented to oxidise readily, producing volatile compounds such as aldehydes and ketones that impart undesirable flavours. Although microencapsulation provided a protective barrier and delayed deterioration, it did not fully prevent oxidation under room temperature storage. Gradual degradation of the wall material or diffusion of oxidation products through the capsule matrix likely contributed to the decline in flavour acceptability. It should also be noted that the chocolates were not stored under inert environmental conditions, which may have accelerated oxidative change.[11]

The results emphasise the importance of enhancing long-term sensory stability for functional chocolate products. Future research should investigate advanced encapsulation techniques using barrier-enhanced materials or multilayered encapsulation systems. Incorporating natural antioxidants such as tocopherols, rosemary extracts, or green tea polyphenols into the encapsulant matrix, combined with optimised storage conditions (*e.g.*, modified atmosphere packaging with inert gases, vacuum sealing, or refrigerated storage), may significantly enhance the oxidative stability and sensory acceptability of omega-3-enriched 3D-printed chocolates. Such approaches are vital to ensuring the sustained consumer acceptance and commercial viability of these innovative functional food products.

4. Conclusion

This study evaluated the influence of the omega-3 form (microencapsulated powder *vs.* oil) and concentration (5%, 10%, 15%) on the physicochemical, rheological, thermal, microstructural, and sensory properties of 3D-printed functional chocolate. All formulations demonstrated excellent printability and structural fidelity, confirming dark chocolate as a suitable matrix for omega-3 enrichment *via* extrusion-based 3D printing. Microscopically, particle aggregation and increased surface roughness were evident at higher powder concentrations (OP10 and OP15), though encapsulation integrity was preserved. Texture analysis revealed a significant dose-dependent softening, with omega-3 oil-containing samples exhibiting the greatest reduction in breaking force compared to the controls, highlighting disruption to cocoa butter crystallisation. Thermally, microencapsulated omega-3 increased

Table 5 Mean ± SD sensory scores (9-point Likert scale) for aroma, taste, and flavour of control and OP10 chocolate after two months of storage ($n = 31$)

Attribute	Control (mean ± SD)	OP10 (mean ± SD)	t (df)	p-Value
Aroma	6.29 ± 1.35	6.19 ± 1.51	−0.2659 (60)	0.7913
Taste	6.00 ± 1.46	5.16 ± 1.88	−1.9606 (60)	0.0546
Flavour	6.00 ± 1.39	4.84 ± 1.93	−2.7146 (60)	0.0087[a]

[a] Indicates significant differences ($p < 0.05$).

melting enthalpy (ΔH) from 44.30 ± 1.69 J g^{-1} (control) up to 57.66 ± 2.02 J g^{-1} (OP15), suggesting enhanced fat crystallinity *via* particle-induced nucleation. Rheological measurements confirmed typical shear-thinning behaviour, showing an initial increase in viscosity at higher powder levels (OP10 and OP15) followed by a viscosity reduction under steady-state shear, indicative of particle-induced lubrication. Sensory evaluation established that freshly printed microencapsulated omega-3 chocolates (OP10) effectively masked off-flavours, achieving comparable acceptability to that of the control ($p > 0.05$). However, flavour scores significantly declined after two months at room temperature under ambient conditions ($p < 0.05$), indicating oxidative instability. Overall, these results affirm microencapsulated omega-3 as a promising approach for functional chocolate 3D printing, provided encapsulation and storage conditions are optimised to maintain long-term sensory quality.

Conflicts of interest

There are no conflicts to declare.

Data availability

The data of this study will be made available to readers upon request.

Acknowledgements

The authors gratefully acknowledge Nu-Mega Ingredients Pty Ltd (Brisbane, Australia) for their provision of raw materials and valuable technical input. We also thank Dr Buddhi Dayananda, Senior Biometric Consultant, School of Agriculture and Food Sustainability, The University of Queensland, for his advice on the statistical analysis and guidance in ensuring appropriate application of methods.

References

1 G. Santos-Sánchez and I. Cruz-Chamorro, Functional Foods as a New Therapeutic Strategy 2.0, *Nutraceuticals*, 2025, **5**(1), 7.
2 S. Wichansawakun, K. Chupisanyarote, W. Wongpipathpong, G. Kaur and H. S. Buttar, in *Functional Foods and Nutraceuticals in Metabolic and Non-communicable Diseases*, ed. R. B. Singh, S. Watanabe and A. A. Isaza, Academic Press, 2022, pp. 533–549.
3 D. Granato, F. J. Barba, D. Bursać Kovačević, J. M. Lorenzo, A. G. Cruz and P. Putnik, Functional Foods: Product Development, Technological Trends, Efficacy Testing, and Safety, *Annu. Rev. Food Sci. Technol.*, 2020, **11**, 93–118.
4 Z. F. Ma, C. Fu and Y. Y. Lee, The Modulatory Role of Bioactive Compounds in Functional Foods on Inflammation and Metabolic Pathways in Chronic Diseases, *Foods*, 2025, **14**(5), 821.
5 A. Abedini, S. Sohrabvandi, P. Sadighara, H. Hosseini, M. Farhoodi, E. Assadpour, M. Alizadeh Sani, F. Zhang, S. Seyyedi-Mansour and S. M. Jafari, Personalized nutrition with 3D-printed foods: A systematic review on the impact of different additives, *Adv. Colloid Interface Sci.*, 2024, **328**, 103181.
6 D. Swanson, R. Block and S. A. Mousa, Omega-3 Fatty Acids EPA and DHA: Health Benefits Throughout Life, *Adv. Nutr.*, 2012, **3**, 1–7.
7 J. K. Innes and P. C. Calder, Marine Omega-3 (N-3) Fatty Acids for Cardiovascular Health: An Update for 2020, *Int. J. Mol. Sci.*, 2020, **21**(4), 1362.
8 T. Shibabaw, Omega-3 polyunsaturated fatty acids: anti-inflammatory and anti-hypertriglyceridemia mechanisms in cardiovascular disease, *Mol. Cell. Biochem.*, 2021, **476**, 993–1003.
9 M. Zeppieri, C. Gagliano, F. D'Esposito, M. Musa, I. Gattazzo, M. S. Zanella, F. B. Rossi, A. Galan and S. Babighian, Eicosapentaenoic Acid (EPA) and Docosahexaenoic Acid (DHA): A Targeted Antioxidant Strategy to Counter Oxidative Stress in Retinopathy, *Antioxidants*, 2025, **14**(1), 6.
10 M. Makrides and R. A. Gibson, Long-chain polyunsaturated fatty acid requirements during pregnancy and lactation123, *Am. J. Clin. Nutr.*, 2000, **71**, 307S–311S.
11 P. Lembke and A. Schubert, in *Omega-3 Fatty Acids in Brain and Neurological Health*, ed. R. R. Watson and F. De Meester, Academic Press, Boston, 2014, pp. 455–460.
12 T. A. Comunian and C. S. Favaro-Trindade, Microencapsulation using biopolymers as an alternative to produce food enhanced with phytosterols and omega-3 fatty acids: A review, *Food Hydrocolloids*, 2016, **61**, 442–457.
13 V. K. Venugopalan, L. R. Gopakumar, A. K. Kumaran, N. S. Chatterjee, V. Soman, S. Peeralil, S. Mathew, D. J. McClements and R. C. Nagarajarao, Encapsulation and Protection of Omega-3-Rich Fish Oils Using Food-Grade Delivery Systems, *Foods*, 2021, **10**(7), 1566.
14 F. C. Godoi, S. Prakash and B. R. Bhandari, in *Engineering Plant-Based Food Systems*, ed. S. Prakash, B. R. Bhandari and C. Gaiani, Academic Press, 2023, pp. 301–314, DOI: 10.1016/b978-0-323-89842-3.00001-4.
15 Z. Liu, M. Zhang, B. Bhandari and Y. Wang, 3D printing: Printing precision and application in food sector, *Trends Food Sci. Technol.*, 2017, **69**, 83–94.
16 S. Koirala, S. Prakash, A. Karim and B. Bhandari, 4D shape morphing in 3D-printed pea protein structures through designed surface grooves under drying and frying conditions, *Innovative Food Sci. Emerg. Technol.*, 2025, 103924, DOI: 10.1016/j.ifset.2025.103924.
17 J. Sun, Z. Peng, W. Zhou, J. Y. H. Fuh, G. S. Hong and A. Chiu, A Review on 3D Printing for Customized Food Fabrication, *Procedia Manuf.*, 2015, **1**, 308–319.
18 F. C. Godoi, B. R. Bhandari, S. Prakash and M. Zhang, *Fundamentals of 3D Food Printing and Applications*, Academic press, 2018.
19 F. C. Godoi, S. Prakash and B. R. Bhandari, 3d printing technologies applied for food design: Status and prospects, *J. Food Eng.*, 2016, **179**, 44–54.
20 E. Pilavci, D. Baykara, K. Ozkan, A. Tiryaki, M. M. Ayran, G. Enguven, T. A. Tut, M. M. Bozdag, O. Sagdic,

O. Gunduz, R. J. Narayan and C. Dogan, ChocOmega-3: Innovative manufacturing of ω-3-enriched chocolate, *Int. J. Bioprint.*, 2024, **10**(6), 3969.

21 P. Rando and M. Ramaioli, Food 3D printing: Effect of heat transfer on print stability of chocolate, *J. Food Eng.*, 2021, **294**, 110415.

22 L. Li and G. Liu, Engineering effect of oleogels with different structuring mechanisms on the crystallisation behaviour of cocoa butter, *Food Chem.*, 2023, **422**, 136292.

23 J. Chen, S. M. Ghazani, J. A. Stobbs and A. G. Marangoni, Tempering of cocoa butter and chocolate using minor lipidic components, *Nat. Commun.*, 2021, **12**, 5018.

24 G. Talbot, in *Cocoa Butter and Related Compounds*, ed. N. Garti and N. R. Widlak, AOCS Press, 2012, pp. 1–33, DOI: 10.1016/B978-0-9830791-2-5.50004-9.

25 O. S. Toker, N. Konar, I. Palabiyik, H. Rasouli Pirouzian, S. Oba, D. G. Polat, E. S. Poyrazoglu and O. Sagdic, Formulation of dark chocolate as a carrier to deliver eicosapentaenoic and docosahexaenoic acids: Effects on product quality, *Food Chem.*, 2018, **254**, 224–231.

26 P. Faccinetto-Beltrán, A. R. Gómez-Fernández, A. Santacruz and D. A. Jacobo-Velázquez, Chocolate as Carrier to Deliver Bioactive Ingredients: Current Advances and Future Perspectives, *Foods*, 2021, **10**(9), 2065.

27 R. L. Milliken, A. Dedeloudi, E. Vong, R. Irwin, S. K. Andersen, M. P. Wylie and D. A. Lamprou, 3D printed cacao-based formulations as nutrient carriers for immune system enhancement, *Curr. Res. Food Sci.*, 2025, **10**, 100949.

28 V.-N. Lesutan, R. L. Milliken, A. Browne, T. Ferguson and D. A. Lamprou, Enhancing 3D-printed chocolate drug delivery: the role of soy lecithin in improving formulation printability and consistency, *RPS Pharm. Pharmacol. Rep.*, 2025, **4**, rqae030.

29 M. Hadnađev, M. Kalić, V. Krstonošić, N. Jovanović-Lješković, T. Erceg, D. Škrobot and T. Dapčević-Hadnađev, Fortification of chocolate with microencapsulated fish oil: Effect of protein wall material on physicochemical properties of microcapsules and chocolate matrix, *Food Chem.: X*, 2023, **17**, 100583.

30 S. Mantihal, S. Prakash, F. C. Godoi and B. Bhandari, Optimisation of chocolate 3D printing by correlating thermal and flow properties with 3D structure modeling, *Innovative Food Sci. Emerg. Technol.*, 2017, **44**, 21–29.

31 Z. Liu, B. Bhandari, S. Prakash, S. Mantihal and M. Zhang, Linking rheology and printability of a multicomponent gel system of carrageenan-xanthan-starch in extrusion based additive manufacturing, *Food Hydrocolloids*, 2019, **87**, 413–424.

32 S. Mantihal, S. Prakash and B. Bhandari, Textural modification of 3D printed dark chocolate by varying internal infill structure, *Food Res. Int.*, 2019, **121**, 648–657.

33 S. Koirala, S. Prakash, A. Karim and B. Bhandari, Shape morphing of food: Designed surface grooves induce controlled 2D-3D-4D shape changes in a pea protein-based product during drying and frying conditions, *Food Struct.*, 2025, **44**, 100433.

34 A. Va, C. T. Udayarajan, G. Goksen, C. S. Brennan and P. Nisha, A brief review on 3D printing of chocolate, *Int. J. Food Sci. Technol.*, 2023, **58**, 2811–2828.

35 M. K. Samota, M. Kaur, S. S. Selvan, R. Kaur, Varinda, A. Ahlawat and M. Kaur, Shaping the future of food: 3D-Printed personalized nutrition and sustainable production pathways, *Food Humanity*, 2025, **4**, 100625.

36 E. O. Afoakwa, A. Paterson, M. Fowler and J. Vieira, Comparison of rheological models for determining dark chocolate viscosity, *Int. J. Food Sci. Technol.*, 2009, **44**, 162–167.

37 E. O. Afoakwa, A. Paterson and M. Fowler, Effects of particle size distribution and composition on rheological properties of dark chocolate, *Eur. Food Res. Technol.*, 2008, **226**, 1259–1268.

38 S. A. C. Agibert and S. C. d. S. Lannes, Dark chocolate with a high oleic peanut oil microcapsule content, *J. Sci. Food Agric.*, 2018, **98**, 5591–5597.

39 H. Meigui, L. Xu, E. Assadpour, C. Tan and S. M. Jafari, Application of nano/micro-encapsulated bioactive compounds in 3D printed foods, *Trends Food Sci. Technol.*, 2025, **158**, 104937.

40 X. Ning, S. Devahastin, X. Wang, N. Wu, Z. Liu, Y. Gong, L. Zhou, L. Huo, W. Ding, J. Yi, C. Guo and X. Hu, Understanding 3D food printing through computer simulation and extrusion force analysis, *J. Food Eng.*, 2024, **370**, 111972.

41 S. B. Gregersen, R. L. Miller, M. Hammershøj, M. D. Andersen and L. Wiking, Texture and microstructure of cocoa butter replacers: Influence of composition and cooling rate, *Food Struct.*, 2015, **4**, 2–15.

42 M. Geary and R. Hartel, Crystallisation Behaviour and Kinetics of Chocolate-Lauric Fat Blends and Model Systems, *J. Am. Oil Chem. Soc.*, 2017, **94**, 683–692.

43 B. J. D. Le Révérend, P. J. Fryer, S. Coles and S. Bakalis, A Method to Qualify and Quantify the Crystalline State of Cocoa Butter in Industrial Chocolate, *J. Am. Oil Chem. Soc.*, 2010, **87**, 239–246.

44 P. Kaushik, K. Dowling, C. J. Barrow and B. Adhikari, Microencapsulation of omega-3 fatty acids: A review of microencapsulation and characterisation methods, *J. Funct. Foods*, 2015, **19**, 868–881.

45 S. M. Ghazani and A. G. Marangoni, Molecular Origins of Polymorphism in Cocoa Butter, *Annu. Rev. Food Sci. Technol.*, 2021, **12**, 567–590.

46 L. Svanberg, L. Ahrné, N. Lorén and E. Windhab, Effect of pre-crystallisation process and solid particle addition on microstructure in chocolate model systems, *Food Res. Int.*, 2011, **44**, 1339–1350.

47 L. Bayés-García, S. Yoshikawa, M. Aguilar-Jiménez, C. Ishibashi, S. Ueno and T. Calvet, Heterogeneous Nucleation Effects of Talc Particles on Polymorphic Crystallisation of Cocoa Butter, *Cryst. Growth Des.*, 2022, **22**, 213–227.